Spatiotemporal variation in the relationship between boreal forest productivity proxies and climate data

Clémentine Ols[1,5*], Ingvil H. Kålås[2,3,6], Igor Drobyshev[1,4], Lars Söderström[3], Annika Hofgaard[2]

[1] Canada Research Chair in Ecology and Sustainable Forest Management, Forest Research Institute, Université du Québec en Abitibi-Témiscamingue, 445 Boulevard de l'Université, J9X5E4 Rouyn-Noranda, QC, Canada

[2] Norwegian Institute for Nature Research, PO Box 5685 Torgarden, NO-7485 Trondheim, Norway

[3] Department of Biology, Norwegian University of Science and Technology, NO-7491 Trondheim, Norway

[4] Swedish University of Agricultural Sciences, Southern Swedish Forest Research Centre, Box 49, 230 53 Alnarp, Sweden

[5] Present address: Institut National de l'Information Géographique et Forestière, Laboratoire d'Inventaire Forestier, 14 rue Girardet, 54000 Nancy, France

[6] Present address: Faculty of Bioscience and Aquaculture, Nord University, NO-7729 Steinkjer, Norway

*Corresponding author: C. Ols ; e-mail: clementine.ols88@gmail.com

Electronic supplementary material The online version of this article contains supplementary material, which is available to authorized users.

Abstract

The impacts of climate change on high-latitude forest ecosystems are still uncertain. Divergent forest productivity trends have recently been reported both at the local and regional level challenging the projections of boreal tree growth dynamics. The present study investigated (i) the responses of different forest productivity proxies to monthly climate (temperature and precipitation) through space and time; and (ii) the local coherency between these proxies through time at four high-latitude boreal Scots pine sites (coastal and inland) in Norway. Forest productivity proxies consisted of two proxies representing stem growth dynamics (radial and height growth) and one proxy representing canopy dynamics (cumulative May-to-September Normalized Difference Vegetation Index (NDVI)). Between-proxy and climate-proxy correlations were computed over the 1982-2011 period and over two 15-yr sub-periods. Over the entire period, radial growth significantly correlated with current year July temperature, and height growth and cumulative NDVI significantly correlated with previous and current growing season temperatures. Significant climate responses were quite similar across sites, despite some higher sensitivity to non-growing season climate at inland sites. Significant climate-proxy correlations identified over the entire period were temporarily unstable. Local coherency between proxies was generally insignificant. The spatiotemporal instability in climate-proxy correlations observed for all proxies underlines evolving responses to climate and challenges the modelling of forest productivity. The general lack of local coherency between proxies at our four study sites suggests that forest productivity estimations based on a single proxy should be considered with great caution. The combined use of different forest growth metrics may help circumvent uncertainties in capturing responses of forest productivity to climate variability and improve estimations of carbon sequestration by forest ecosystems.

Keywords: Dendroclimatology; Remote sensing; Carbon sequestration; Boreal ecosystems; Vegetation productivity; Arctic amplification.

Introduction

In Northern Europe, terrestrial temperature and precipitation have increased over the 20th century and particularly since the late 1980s (IPCC 2014, Hanssen-Bauer et al. 2015). Temperature and precipitation are primary determinants of vegetation growth. Long-term trends in both climate parameters are expected to modify vegetation productivity dynamics (Larsen 1971; Hofgaard et al. 1999). Recent warming has been reported to cause changes in tree phenology (Karlsen et al. 2009) and has induced an increased photosynthetic activity (Buitenwerf et al. 2015). Further, forest productivity in temperature-limited boreal ecosystems has been expected to increase in response to warming conditions (Qian et al. 2010; Stinziano and Way 2014). However, such forecast has been challenged by a recent diversification of forest productivity responses (both positive and negative) to climate warming at northern latitudes (Charney et al. 2016; Hellman et al. 2016, Piao et al. 2011).

Forest productivity can be divided into below (root system dynamics) and above ground components (tree stem and canopy dynamics), the latter being more easily accessible and quantifiable. Common proxies for above-ground forest productivity are radial growth, height growth and Normalized Difference Vegetation Index (NDVI). These have been widely used to study the effects of climate change on forest ecosystems (Mathisen and Hofgaard 2011, Solberg et al. 2002, Du et al. 2014, Pettorelli et al. 2005; Beck et al. 2007, Raynolds et al. 2008; Santin-Janin et al. 2009; Berner et al. 2013). NDVI is a remote sensing measure of ground surface reflectance in visible and near-infrared light available since the early 1980s (Weier and Herring 2000). Healthy growing vegetation, through photosynthetic activity, absorbs most of the visible light and reflects most of the near infrared light, resulting in high NDVI values (Tucker 2004; Pettorelli et al. 2005; Beck et al. 2007). Vegetation productivity is therefore generally positively associated to NDVI (Pettorelli et al. 2005; Santin-Janin et al. 2009).

Divergent forest productivity trends have recently been reported both at the local and regional level (Kaufmann et al. 2004; Lapenis et al. 2005; Beck et al. 2013). These divergences may directly emerge from the use of different proxies and the different physiological processes these latter are

linked to (Marchand et al. 2018). While radial and height growth are mainly linked to xylem formation (tree stem dynamics), NDVI mostly measures photosynthetic activity (canopy dynamics). Knowledge of how tree-stem and canopy dynamics interact and how these interactions may evolve in the face of climate change is limited. To better understand current and future impacts of climate warming on carbon sequestration in forest ecosystems, it is therefore of crucial importance to investigate temporal changes in climate-growth relationships of different productivity proxies and their local coherency through time.

Growth of Scots pine (*Pinus sylvestris* L.), one of the major conifer tree species in Europe, is frequently used as an estimate of high-latitude forest productivity (Berner et al. 2011). In boreal and sub-arctic regions, radial growth of Scots pine correlates with current-year summer temperature (Björklund et al. 2013), July temperature being the strongest monthly determinant (Briffa et al. 1992; Lindholm et al. 1996; Henttonen et al. 2014). Scots pine's height growth primarily correlates with previous summer climate, previous July temperature being the strongest monthly determinant (Lindholm et al. 2009, Mathisen and Hofgaard 2011, Salminen and Jalkanen 2005). The strongest correlations between monthly NDVI and respective monthly temperature fields are primarily observed during warmest months (Potter and Brooks 1998, Seftigen et al. 2018). Despite the dominant control of previous and current summer temperatures on Scots pine's tree stem growth and canopy dynamics, the nature of this control (strength and sign) may vary through both time and space (Büntgen et al. 2009, Mathisen and Hofgaard 2011, Hofgaard et al. 2018). The late 20th century has been characterized by a decreasing correlation between radial growth and temperature in many boreal regions (D'Arrigo et al. 2008; Büntgen et al. 2009; Linderholm et al. 2010). However, whether such a divergence occurs in respect to other forest productivity proxies remains poorly investigated (but see Piao et al. 2014).

In the present study, we investigated recent relationships between above-ground forest productivity and local climate at four high-latitude boreal Scots pine sites in Norway over the 1982-2011 period. Forest productivity proxies consisted of radial growth, height growth, and NDVI.

Three different hypotheses were tested: i) all proxies correlate positively with growing season climate reflecting a stimulating effect of warmer temperature on photosynthesis and tree growth physiological processes; ii) tree stem proxies (radial and height growth) correlate positively with NDVI reflecting the link between carbon source (photosynthesis) and carbon sink (tree growth); and that iii) correlations between proxies are spatially coherent reflecting common climatic drivers on forest productivity.

Methods

Sampling sites

The study was carried out in two regions situated in the northern boreal vegetation zone in Norway (sensu Moen 1999), one approximately three degrees north (N) and one three degrees south (S) of the Arctic Circle [61-70°N, 9-30°E]. In each study region, two forest sites were selected, one representing coastal conditions and one representing more continental inland conditions (Fig. 1a, Table S1). Henceforward sites are named N-coast, N-inland, S-coast and S-inland. At each site, trees from two to three mesic forest stands were selected and sampled for radial and height growth. Selected stands were smaller than 1 ha in size and had no signs of recent disturbance, except few old stumps indicating former selective harvests. The tree layer at all sites was dominated by Scots pine with some scattered birch (*Betula pubescens* Ehrh.). Dwarf shrubs and bryophytes dominated the forest floor of all stands. Soil characteristics at all sites can be described as podsols (European Soil Bureau Network European Commission, 2005) with a bedrock of ancient Precambrian granites and gneisses covered by younger Quaternary sediments (Table S1, geo.ngu.no). Site index at our sampling sites was estimated to range between 6 and 17 by a recent study based on the Norwegian national forest inventory dataset (Antón-Fernández et al. 2016).

In the study regions, coastal climate is generally characterized by moist mean annual conditions (annual precipitation between 950 and 1800 mm) and mild winters (mean winter [DJF] temperature between -6.5 and -3.5°C), while inland climate shows drier mean annual conditions (annual precipitation between 500 and 750 mm) and colder winters (mean winter temperature between -11

and -9.5 °C) (Moen 1999, Table S1). Both coastal and inland climate are under the influence of the North Atlantic Ocean, with decreasing influence moving inland wards.

Climate data

Temperature and precipitation data were obtained from the Norwegian meteorological institute (Norwegian Meteorological Institute 2014, http://sharki.oslo.dnmi.no). For each sampling site, monthly mean temperature and monthly total precipitation data for the 1982-2011 period were acquired both as climate station data and as 1 km^2 resolution grid data (Tveito et al. 2005). Climate stations were selected as close as possible to the sampling sites, with the average and maximum site-station distances being 55 km and 70 km for temperature and 29 km and 40 km for precipitation (Table S3). Grid data were compared with local climate station data (Table S3). Correlations were generally high for all months and for both temperature and precipitation (Table S3). Because the distance between sites and stations, and the period covered by climate station data varied across sites (Table S3), climate-growth analyses were based on grid data. Trends in seasonal mean temperature and total precipitation over the 1982-2011 period were investigated by linear regression. Seasons included spring (MAM), summer (JJA), autumn (SON) and winter (DJF). Trends in summer temperature were significant ($P < 0.05$) at all sites (Appendix A). Further details regarding climate characteristics and trends analyses are given in Appendix A (Figs. S1-S2 and Tables S1-S3).

NDVI data

The selected NDVI dataset consisted of biweekly measurements of the Advanced Very High Resolution Radiometer (AVHRR) produced by the Global Inventory Modeling and Mapping Studies (GIMMS) group at the NASA Goddard Space Flight Centre (NASA 2014). This data set is derived from a fixed grid map with a spatial resolution of 8 km x 8 km. It is readjusted for orbital drift, sensor degradation, cloud cover and aerosols, and characterizes the photosynthetic activity of

vegetated land north of latitude 45° for the 1982-2011 period (Barichivich et al. 2013; Pinzon and Tucker 2014). We computed monthly and cumulative May-to-September NDVI values for each site. Late spring to early autumn (May to September) monthly NDVI were calculated as mean value of the two biweekly observations available per month. Cumulative NDVI was computed as the sum of May-to-September monthly NDVI. Trends in cumulative NDVI over the 1982-2011 period were analysed by linear regression.

Field sampling and data preparation

Tree stem dynamics can be divided into radial growth and height growth components. Under natural conditions, tree stem growth is mainly driven by height growth at young stages (competition for dominant status), and by radial growth when trees have reached a dominant status within a forest stand (Niklas 1995). This is particularly true in uneven-aged natural forests encountered across northern Norway (Mathisen & Hofgaard 2011). In order to describe both radial and height growth allocation in our sampling stands, we chose to sample young trees for height growth and adult trees for radial growth. This sampling strategy had two advantages: (i) it captured tree growth dynamics in a more comprehensive way than height or radial growth alone; (ii) it allowed the study of radial and height growth responses to climate separately, by respectively minimizing the presence of radial growth signals in height growth series and vice versa. Radial and height growth data was sampled at all sampling sites between mid-August and mid-September 2012.

For radial growth, two cores of perpendicular directions were extracted from 30 trees per site, at approximately 130 cm above ground (Fig. 1b). Sampled trees were canopy-dominant healthy mature trees with no visible crown or stem damages. Trees presenting eccentric stem shapes were not sampled. Cores were glued on wooden support and brought to the laboratory, where they were planed with a scalpel to facilitate ring identification. Cores were then scanned at a 1200 dpi resolution and scans imported into CooRecorder (Larsson 2012a) for ring-width measurements. At last, radial series were visually and statistically crossdated at site level using CDendro (Larsson

2012b) and COFECHA 6.06P (Holmes et al. 1986). Nine radial series could not be properly measured and crossdated (series of narrow rings impossible to distinguish) and had to be excluded from further analyses. The number of radial series per site ranged between 55 and 60 (Table 1). Trees at northern sites had a larger mean ring width (mean 1.38 mm) than at southern sites (mean 0.69 mm) (Table 1).

For height growth, 40 young trees growing in canopy gaps were sampled per site (Fig. 1c). The sampling took place in canopy gaps to minimize competition-related effects on growth. Sampled individuals were 130 to 430-cm tall. Annual height growth was recorded with a ruler (0.5 cm accuracy) as the distance between annual branch nodes along the stem. To increase data quality, the sampling aimed for a minimum of 10 trees with no signs of stem damage for each calendar year of the 1982-2011 period covered by NDVI data. This objective was reached at all sites, except at S-coast where two stem-damaged trees had to be included in the measurements. These two trees presented damages in 1991 and 1997, respectively - both damages being likely caused by moose browsing. For these trees, the damaged years and the three following years (considered as a growth recovery period (Mathisen & Hofgaard 2011) - respectively 1991-1994 and 1997-2000) were excluded from the analyses. This resulted in 17 to 31 trees per site and good data coverage for the 1982-2011 period for all sites (Table 1; for annual sample depth variation see Fig. S5). Mean annual height growth varied between 8.25 cm (S-coast) and 9.05 cm (N-inland) (Table 1).

Chronology construction and standardization

All radial and height series were standardized (removal of age-related signals) using R dplR package (R Core Team 2012; Bunn et al. 2014). The standardisation process consisted of a modified negative exponential function to filter out low-frequency signals (Fritts 1976, Cook and Kairiukstis 1990). To study the effect of the detrending method on climate-growth relationships, series were also detrended using a spline function with a 50% variance cut-off equal to two-thirds of the series length (Cook & Peter 1981) and a horizontal line (series' mean). These two other types of

detrending retained as much (for the horizontal line) or less (for the spline) climate signals than the negative exponential detrending (see Appendix B - Figs. S4-S7 and Tables S4-S5), and were thus disregarded from further analyses. Tree ring-width indices were computed as ratios regardless of the detrending method used. Standardized radial series (two per tree) were aggregated into individual tree-level radial series by robust bi-weighted mean. Autocorrelation was removed from radial and height series by autoregressive modelling (order selection done by minimizing AIC) (Cook and Kairiukstis 1990). Finally, radial and height series were averaged into site-specific radial and height growth chronologies by bi-weighted robust mean (Cook and Kairiukstis 1990).

Statistical analyses

The quality of site-specific chronologies was evaluated using correlations among individual tree series (Rbar), expressed population signal (EPS) and signal-to-noise ratio (SNR) in R package dplR (Bunn et al. 2014). The EPS reflects how well the average of all individual tree series represents a theoretically infinite population (Wigley et al. 1984, Buras 2017). The SNR compares the level of signal versus noise in a time series, the higher the SNR, the stronger signal in the series.

Correlations between site-specific proxies (radial, height and cumulative NDVI) and monthly climate variables over the 1982-2011 period were tested by Pearson correlation analyses (Zang and Biondi 2015). Climate variables included monthly mean temperature and monthly total precipitation spanning from previous may (May_{t-1}) to current year August ($August_t$) (16 months in total). To investigate the temporal consistency in significant climate-growth correlations identified over the entire 1982-2011 period, bootstrapped (n = 1000) correlation analyses were computed over two 15-yr sub-periods, namely the 1982-1996 and 1997-2011 period. The significance level was set to 0.05 in all statistical tests, and all climate-growth analyses were run in R using the *treeclim* package (Zang & Biondi, 2015).

The site-specific coherency between proxies was examined by stationary Pearson correlations over the 1982-2011 period. Each correlation was tested for significance using bootstrapped confidence

intervals with 1000 iterations. In addition, we also investigated the temporal consistency between proxies using bootstrapped Pearson correlations computed over the two 15-yr sub-periods mentioned above. Finally, we investigated the correlation between tree stem proxies (radial and height growth) and monthly NDVI, with months spanning from May to September.

Results

Characteristics of the forest productivity proxies

Standardized radial chronologies contained strong common signals (EPS ranging from 0.91 to 0.94 and SNR from 9.7 and 19.8), although values were lower at northern sites than at southern sites (Table 1). Height chronologies had less common signals than radial chronologies (EPS ranging from 0.77 to 0.89 and SNR from 3.3 and 8.3), and presented lower values at inland sites than at coastal sites (Table 1). Site-specific mean correlation between all standardized individual tree series ranged between 0.24 and 0.48 for radial growth and between 0.18 and 0.32 for height growth (Table 1). Cumulative NDVI series presented significant positive trends over the 1982-2011 period at S-inland (+0.0143 yr^{-1}) and at N-coast (+0.0118 yr^{-1}) (Fig. 2).

Correlations between forest productivity proxies and monthly temperature

Radial growth

Radial growth significantly and positively correlated with $July_t$ temperature at southern sites (Fig. 3). Sub-period correlation analyses revealed that this correlation with $July_t$ was restricted to the first sub-period (1982-1996) (Fig. 4). Additional significant correlations over the full period were all negative and observed with $July_{t-1}$ at N-coast, with $August_{t-1}$ at N-inland and with $February_t$ at S-inland (Fig. 3). These negative correlations were mostly non-significant when computed at the sub-period level, except for the correlation with $July_{t-1}$ at N-coast during the first sub-period (Fig. 4).

Height growth

Significant positive correlations between height growth and temperature over the full period were observed with May_{t-1}-$September_{t-1}$ and $April_t$-$August_t$ temperatures at most sites, with significant correlations with $July_{t-1}$ and $August_{t-1}$ at all sites (Fig. 3). Additional significant correlations (all positive) were observed with $November_{t-1}$ at N-inland and $March_t$ at S-coast (Fig. 3). During the first sub-period, positive significant associations were mostly observed with $July_{t-1}$ and $August_{t-1}$ temperature at all sites except at S-coast (Fig. 4). During the second sub-period, these climate-growth associations showed similar pattern across sites although not all significant. Numerous shifts from non-significant to significant positive correlations were observed at S-coast during both previous and current growing season months (Fig. 4).

Cumulative NDVI

Significant correlations between cumulative NDVI and temperature over the full period were mostly positive and observed during $June_{t-1}$-$August_{t-1}$ and $April_t$-$August_t$, although not consistent across sites (Fig. 3). In addition to these general positive correlations, significant correlations were also observed with $February_t$ (positive) at S-coast and with $October_{t-1}$ (negative) at S-inland (Fig. 3). At the sub-period level, the sign of these individual correlations remained mostly unchanged over both sub-periods (either stayed positive or negative) but their level of significance was unstable (Fig. 4).

Correlation between forest productivity proxies and monthly precipitation

Radial growth

Over the 1982-2011 period, significant correlations between radial growth and monthly precipitation were mostly observed at southern sites (Fig. 3). Significant correlations were found positive with $October_{t-1}$, $January_t$ and $August_t$ at S-inland, and negative with $September_{t-1}$ and $October_{t-1}$ at S-coast. An additional significant positive correlation with $July_{t-1}$ was observed at N-coast (Fig. 3). At the sub-period level, the sign of these individual correlations remained unchanged, but their level of significance was unstable (Appendix C - Fig. S9).

Height growth

Over the entire period, significant correlations between height growth and monthly precipitation were observed with $September_{t-1}$ (positive) at N-coast, with May_{t-1}, $December_{t-1}$, $March_t$ and $April_t$ (all positive) at N-inland, with $July_{t-1}$ (negative) at S-coast and with $July_t$ (positive) at S-inland (Fig. 3). At the sub-period level, these correlations presented the same sign but became all non-significant, except for the positive associations with May_{t-1} and $April_t$ at N-inland that were significant during the first and second sub-period, respectively (Appendix C - Fig. S9).

Cumulative NDVI

Over the 1982-2011 period, significant correlations between cumulative NDVI and monthly precipitation were observed with $August_{t-1}$ (positive) at southern sites and with $August_t$ (negative) at N-coast (Fig. 3). Between the first and the second sub-period, the signs of these correlations remained unchanged and their significance level changed from being non-significant to significant at southern sites and vice versa at N-coast (Appendix C - Fig. S9).

Local coherency between forest productivity proxies

Over the 1982-2011 period, very few significant correlations were observed between proxies at site level. Radial growth correlated negatively with height growth at N-inland ($r = -0.44$), height growth correlated positively and significantly with cumulative NDVI at N-coast ($r = 0.47$) and S-inland ($r = 0.34$) (Table 2). Over the two sub-periods, the sign of these correlations remained unchanged. The negative correspondence between radial and height growth was only significant during the second sub-period while the correspondence between height growth and cumulative NDVI was only significant during the first sub-period (Fig. 5). Sub-period analyses revealed an additional significant positive correlation between height growth and cumulative NDVI at S-coast during the first sub-period (Fig. 5). Correspondence analyses between monthly NDVI and tree stem growth proxies revealed that radial growth correlated significantly with May and June NDVI at N-coast, and with June NDVI at N-inland (all negative). Height growth correlated significantly with August

NDVI at N-coast, with May NDVI at S-coast and with September NDVI at S-inland (all positive) (Appendix D – Fig. S10).

Discussion

Climate responses of individual proxies through space

Radial growth was mainly controlled by late summer temperatures at most of the sites, as generally assumed for high latitudes boreal forests (Briffa et al. 1992; Lindholm et al. 1996; Drobyshev et al. 2004; Henttonen et al. 2014). Radial growth was also influenced by non-growing season precipitation at southern sites. This influence was negative at the coastal site and positive at the inland site. Autumn and winter precipitation favour snow accumulation and subsequently soil insulation during cold months protecting finer roots from frost damages, and contributing to essential meltwater during early growing-season. This protection and source of water is probably particularly important in colder and dryer winter inland conditions (Vaganov et al. 1999, Sturm et al. 2001, Fréchette et al. 2011). In addition, radial growth was positively associated with previous and current summer precipitation at two sites, underlining the needs and importance of soil water inputs in physiological growth processes during the growing season (Sands & Mulligan 1990).

The spatially-consistent positive response of height growth to previous and current growing season temperature is in line with previously reported temperature-height growth response in northern Fennoscandia (Junttila and Heide 1981; Mathisen and Hofgaard 2011). The number of cells produced during bud initiation at the end of the previous growing season, and used for stem elongation in the following year, are positively controlled by temperature (Lanner 1968; Lanner 1985). The positive significant responses of height growth to non-growing season temperature observed at N-inland may emerge from higher temperatures being naturally associated with higher precipitation levels during the non-growing season in our study region (Appendix A - Fig. S3). Higher precipitation levels during the dormant season may favour snow accumulation and provide

height growth with better melt water availability at the start of the stem elongation period, particularly at drier inland regions and this regardless of soil characteristics.

Cumulative NDVI responded positively and significantly to previous and current spring and summer temperatures at all sampled sites, and generally did not respond to precipitation – except at N-coast where it significantly and negatively correlated with late summer precipitation. These results indicate a stimulating effect of higher temperature on photosynthetic activity (Kramer 1982) and reveal that NDVI responses to growing season climate are present, contrarily to a recently reported divergence observed at other northern boreal regions (Piao et al. 2014). Cumulative NDVI presented significant negative responses to non-growing season temperatures at inland sites. Photosynthetic activity during the dormancy period has been reported to cause minimal loss of carbon reserves for Scots pine (Hansen et al. 1996). However, in the face of recent warming, a temperature threshold might have been reached whereby an increased photosynthetic activity in response to a warmer dormancy climate would cause a significant depletion in carbon reserves and a lower rate of needle production in the following growing season.

Climate-growth relationships of individual proxies through time

The dominant effect of late summer temperature on radial growth was not temporally consistent. This inconsistency questions climate reconstructions that are elaborated assuming temporally stable relationships between a proxy and climate variables (Luterbacher et al. 2016). Taking into account the non-stationarity nature of climate-growth relationships would improve the reliability of such reconstructions, but would require a deeper understanding of what drives changes in trees' sensitivity to climate (Hofgaard et al. 2018).

The consistent positive correlation between height growth and $August_{t-1}$ temperature observed at all sites but the southern coastal site at the sub-period level, underlines that despite significant summer warming height growth remains temperature-limited at high latitudes (Lindholm et al. 2009, Mathisen and Hofgaard 2011, Salminen and Jalkanen 2005). This dominant control of

temperature on height growth was also underlined by emergent significant correlations between height growth and summer temperature at the southern coastal site during the second sub-period.

The consistent correlation pattern between cumulative NDVI and growing season temperatures observed at sub-period level contradicts to some extent a reported decline in the relationship between growing season temperature and vegetation productivity at boreal latitudes between 1982 and 2011 (Piao et al. 2014). In a context of climate warming, the stable positive correspondence between temperature and NDVI might indicate an acclimation of photosynthetic temperature optima (Sendall et al. 2015). However, non-linear responses of NDVI to temperature (Zhou et al. 2003) may, in a near future, hamper or cancel out the herein observed positive temperature-NDVI relationship.

Local coherency between proxies

The generally insignificant coherency between proxies revealed in this study is in line with previously reported results for boreal conifer trees (Kaufmann et al. 2004; Lapenis et al. 2005; Mathisen and Hofgaard 2011; Beck et al. 2013, Brehaut and Danby 2018).

The general lack of significant correlation between radial and height growth observed at all sites, but the northern inland site, can likely be explained by different climate sensitivity of these proxies. On one side, radial growth is constrained by the number and size of vascular cells produced during the current growing season, and is therefore most sensitive to current year summer temperature (Vaganov et al. 2011, Cuny et al. 2013). On the other side, height growth (bud cell elongation) depends on the number of bud cells produced the previous year at the end of the growing season and on elongation conditions during current growing season, and is therefore most sensitive to previous year late summer temperature and to early growing season climate (Lanner 1968; Lanner 1985). However, the significant negative correlation observed between radial and height growth at the northern inland site may suggest that at stand level physiological processes linked to these two proxies are antagonists due to resource limitations and competition level.

Accordingly, available resources may be predominantly allocated either to radial or height increment depending on the competition status of a tree within the stand.

The lack of correlation between radial growth and cumulative NDVI observed may directly emerge from cumulative NDVI masking monthly interactions between tree-stem growth and photosynthetic activity dynamics. Hypothetically radial growth, mainly limited by late summer temperature, would correlate with late summer monthly NDVI. However, significant correlations between radial growth and monthly NDVI were instead observed with early summer monthly NDVI (May and June) and these were all negative and limited to northern sites (Appendix D – Fig. S10). Results therefore indicate that radial growth appears decoupled from growing season canopy dynamics at our sampled sites. This decoupling further suggests, assuming that NDVI is a good proxy for photosynthetic activity and for carbon sequestration, that the proportion of recently assimilated carbon allocated to radial growth varies through time (at monthly and annual scale). This temporal variability might be linked to changes in other growth-limiting constraints, such as massive seeds production (Koenig et al. 1998, Roland et al. 2014) or soil moisture conditions (Oberhuber et al. 2011). The negative correlations between radial growth and early summer monthly NDVI observed at northern sites may further suggest that radial growth could emerge from the use of carbon reserves, e.g. non-structural carbohydrates (Vargas et al. 2009, Oberhuber et al. 2011, Ols et al. 2016), even during periods of high photosynthetic activity. This hypothesis could also be supported by the higher sensitivity of radial growth to previous summer than to current summer months at northern sites.

The significant and positive correlation between height growth and cumulative NDVI at two sites (N-coast and S-inland) over the entire 1982-2011 period could possibly be explained by similar positive responses to previous and current year growing season temperatures. However, the significance of this correlation was unstable through time, revealing complex non-linear interactions between height growth and canopy dynamics in the study area.

The general lack of coherency between NDVI and tree stem dynamics (radial and height growth) may also be linked to the spatial resolution (8km x 8km) of the herein used NDVI dataset. The spatial coverage of each site-specific NDVI not only encompasses the site per se but also diverse surrounding land cover types.

Conclusions

The local incoherency between forest productivity proxies observed in the present study suggests that forest productivity trends based on single-proxy estimations should be considered with great caution. Spatiotemporal asynchrony across forest productivity proxies may further increase due to instable responses to climate. In addition, the ongoing rapid climate change puts trees in the face of unprecedented growing conditions and increases the level of complexity of interactions between tree growth compartments. The recent development of remote sensing products with higher spatial resolution is a promising path towards unravelling the physiological links between tree stem and canopy dynamics and estimating the future carbon sequestration capacity of forest ecosystems.

Acknowledgements This work is a product under the NINA's strategic institute program portfolio and the PREREAL project funded by the Research Council of Norway (grant no. 160022/F40 and 260400/E10; AH), and part of NordicDendro, a Nordic-Canadian network on forest growth research, supported by Nordic Council of Ministers (grant no. 12262; ID). We thank Rakel J. Alvestad for assistance at the field site in Pasvik, and the anonymous reviewers for their helpful and constructive comments on previous versions of this manuscript.

References

1. Antón-Fernández C., Mola-Yudego B., Dalsgaard L., Astrup R., 2016. Climate-sensitive site index models for Norway. Can. J. For. Res. 46, 794–803.
2. Barichivich J., Briffa K.R., Myneni R.B., Osborn T.J., Melvin T.M., Ciais P., Piao S., Tucker C., 2013. Large-scale variations in the vegetation growing season and annual cycle of

atmospheric CO2 at high northern latitudes from 1950 to 2011. Glob. Chang. Biol. 19, 3167–3183.

3. Beck P.S.A., Jönsson P., Høgda K.A., Karlsen S.R., Eklundh L., Skidmore A.K., 2007. A ground-validated NDVI dataset for monitoring vegetation dynamics and mapping phenology in Fennoscandia and the Kola Peninsula. Int. J. Remote Sens. 28, 4311–4330.
4. Beck P.S.A., Andreu-Hayles L., D'Arrigo R., Anchukaitis K.J., Tucker C.J., Pinzón J.E., Goetz S.J., 2013. A large-scale coherent signal of canopy status in maximum latewood density of tree rings at arctic treeline in North America. Glob. Planet. Chang. 100, 109–118.
5. Berner L.T., Beck P.S.A., Bunn A.G., Lloyd A.H., Goetz S.J., 2011. High-latitude tree growth and satellite vegetation indices: Correlations and trends in Russia and Canada (1982-2008). J. Geophys. Res. 19, 116, G01015, doi:10.1029/2010JG001475.
6. Berner L.T., Beck P.S.A., Bunn A.G., Goetz S.J., 2013. Plant response to climate change along the forest-tundra ecotone in northeastern Siberia. Glob. Chang. Biol. 19, 3449–3462.
7. Björklund J.A., Gunnarson B.E., Krusic P.J., Grudd H., Josefsson T., Östlund L., Linderholm H.W., 2013. Advances towards improved low-frequency tree-ring reconstructions, using an updated *Pinus sylvestris* L. MXD network from the Scandinavian Mountains. Theor. Appl. Climatol. 113, 697–710.
8. Brehaut L., Danby R.K., 2018. Inconsistent relationships between annual tree ring-widths and satellite-measured NDVI in a mountainous subarctic environment. Ecol. Indic. 91: 698-711.
9. Buitenwerf R., Rose L., Higgins S.I., 2015. Three decades of multi-dimensional change in global leaf phenology. Nat. Clim. Chang. 5, 364–710
10. Bunn A.M.K., Biondi F., Campelo F., Mérian P., Mudelsee M., Qeadan F., Schulz M., Zang C., 2014. dplR: Dendrochronology Program Library in R. R package version 1.5.8.
11. Büntgen U., Wilson R., Wilmking M., Niedzwiedz T., Bräuning A., 2009. The 'Divergence Problem' in tree-ring research. TRACE 7, 212–219.
12. Buras A., 2017. A comment on the expressed population signal. Dendrochronologia 44, 130–132.
13. Briffa K.R., Jones P.D., Schweingruber F.H., 1992. Tree-ring density reconstructions of summer temperature patterns across western North-America since 1600. J. Clim. 5, 735–754.
14. Charney N.D., Babst F., Poulter B., Record S., Trouet V.M., Frank D., Enquist B.J., Evans M.E., 2016. Observed forest sensitivity to climate implies large changes in 21st century North American forest growth. Ecol. Lett. 19, 1119–1128.

15. Cook E.R., Kairiukstis L.A. (eds.), 1990. Methods of dendrochronology: Applications in the environmental sciences. Springer Science & Business Media BV. Springer Netherlands.
16. Cook, E.R. & Peters, K., 1981. The smoothing spline: a new approach to standardizing forest interior tree-ring width series for dendroclimatic studies. Tree-Ring Bull. 41, 45-53.
17. Cuny H.E., Rathgeber C.B., Kiesse T.S., Hartmann F.P., Barbeito I., Fournier M., 2013. Generalized additive models reveal the intrinsic complexity of wood formation dynamics. J. Exp. Bot. 64 (7), 1983–94.
18. Drobyshev I., Niklasson M., Angelstam P., 2004. Contrasting tree-ring data with fire record in a pine-dominated landscape in Komi republic (Eastern European Russia): recovering a common climate signal. Silva Fenn. 38, 43–53.
19. Du J., He Z., Yang J., Chen L., Zhu X., 2014. Detecting the effects of climate change on canopy phenology in coniferous forests in semi-arid mountain regions of China. Int. J. Remote Sens. 35, 6490–6507.
20. European Soil Bureau Network European Commission. 2005. Soil Atlas of Europe. Office for Official Publications of the European Communities, L-2995 Luxembourg, 128 pp.
21. Fréchette E., Ensminger I., Bergeron Y., Gessler A. & Berninger F., 2011. Will changes in root-zone temperature in boreal spring affect recovery of photosynthesis in *Picea mariana* and *Populus tremuloides* in a future climate? Tree. Physiol. 31**,** 1204–1216.
22. Fritts H.C., 1976. Tree rings and climate. Academic Press, London.
23. Hansen J., Vogg G., Beck E., 1996. Assimilation, allocation and utilization of carbon by 3-year-old Scots pine (*Pinus sylvestris* L.) trees during winter and early spring. Trees 11, 83–90.
24. Hanssen-Bauer I., Drange H., Førland E.J., Roald L.A., Børsheim K.Y., Hisdal H., Lawrence D., Nesje A., Sandven S., Sorteberg A., 2015. Klima i Norge 2100. Kunnskapsgrunnlag for klimatilpasning oppdatert 2015. Norsk klimaservicesenter rapport no. 2/2015, pp. 1–204.
25. Hellmann, L., Agafonov, L., Ljungqvist, F. C., Churakova, O., Düthorn, E., Esper, J., … Büntgen, U. (2016). Diverse growth trends and climate responses across Eurasia's boreal forest. Environ Res Lett, 11(7), 074021. https://doi.org/10.1088/1748-9326/11/7/074021
26. Henttonen H.M., Mäkinen H., Heiskanen J., Peltoniemi M., Laurén A., Hordo M., 2014. Response of radial increment variation of Scots pine to temperature, precipitation and soil water content along a latitudinal gradient across Finland and Estonia. Agric. For. Meteorol. 198, 294–308.

27. Hofgaard A., Tardif J., Bergeron Y., 1999. Dendroclimatic response of *Picea mariana* and *Pinus banksiana* along a latitudinal gradient in the eastern Canadian boreal forest. Can. J. For. Res. 29, 1333–1346.
28. Hofgaard A., Ols **C**., Drobyshev I., Kirchhefer A.J., Standberg S., Söderström L. 2019. Non-stationary response of tree growth to climate trends along the Arctic margin. *Ecosystems*. 22: 434-451.
29. Holmes R.L., Adams R.K., Fritts H.C., 1986. Tree-ring chronologies of western North America: California, eastern Oregon and northern Great Basin, with procedures used in the chronology development work, including users manuals for computer programs COFECHA and ARSRAN. Chronology Series VI. University of Arizona, Tucson, Arizona.
30. IPCC, 2014. Intergovernmental Panel on Climate Change. Climate Change 2014: Synthesis Report. Contribution of Working Groups I, II and III to the Fifth Assessment Report of the Intergovernmental Panel on Climate Change ed Pachauri RK and Meyer LA. Geneva, pp. 1–151.
31. Junttila O., Heide O.M., 1981. Shoot and needle growth in *Pinus sylvestris* as related to temperature in northern Fennoscandia. For. Sci. 27, 423–430.
32. Karlsen S.R., Høgda K.A., Wielgolaski F.E., Tolvanen A., Tømmervik H., Poikolainen J., Kubin E., 2009. Growing-season trends in Fennoscandia 1982–2006, determined from satellite and phenology data. Clim. Res. 39, 275–286.
33. Kaufmann R.K., D'Arrigo R.D., Laskowski C., Myneni R.B., Zhou L., Davi N.K., 2004. The effect of growing season and summer greenness on northern forests. Geophys. Res. Lett. 31, 09205.
34. Kirchhefer A.J., 2001. Reconstruction of summer temperatures from tree-rings of Scots pine (*Pinus sylvestris* L.) in coastal northern Norway. Holocene 11, 41–52
35. Koenig W.D. & Knops J.M.H., 1998. Scale of mast-seeding and tree-ring growth. Nature 396, 225–226.
36. Kramer P.J., 1982. Water and plant productivity of yield, in Handbook of Agricultural Productivity, edited by Rechcigl M, CRC Press, Boca Raton, Fla, pp. 41–47.
37. Lanner R.M., 1968. The pine shoot primary growth system. University of Minnesota, Minnesota.
38. Lanner R.M., 1985. On the insensitivity of height growth to spacing. For. Ecol. Manage. 13, 143–148.
39. Lapenis A., Shvidenko A., Shepaschenko D., Nilsson S., Aiyyer A., 2005. Acclimation of Russian forests to recent changes in climate. Glob. Chang. Biol. 11, 2090–2102.

40. Larsen J.A., 1971. Vegetational relationships with air mass frequencies - Boreal forest and tundra. Arctic 24, 177–194.
41. Larsson L.-Å., 2012a. Cybis CooRecorder. CybisElktronik & Data AB, Saltsjöbaden.
42. Larsson L.-Å., 2012b. CDendro: Cybis Dendro dating program, CybisElktronik & Data AB, Saltsjöbaden.
43. Linderholm H.W., Björklund J.A., Seftigen K., Gunnarson B.E., Grudd H., Jeong J.H., Drobyshev I., Liu Y., 2010. Dendroclimatology in Fennoscandia - from past accomplishments to future potential. Clim. Past. 6, 93–114.
44. Lindholm M., Timonen M., Meriläinen J., 1996. Extracting mid-summer temperatures from ring-width chronologies of living pines at the northern forest limit in Fennoscandia. Dendrochronologia 14, 99–113.
45. Lindholm M., Ogurtsov M., Aalto T., Jalkanen R., Salminen H., 2009. A summer temperature proxy from height increment of Scots pine since 1561 at the northern timberline in Fennoscandia. Holocene 19, 1131–1138.
46. Luterbacher J., Werner J.P., Smerdon J.E., Fernández-Donado, L., González-Rouco, F.J., Barriopedro, D., Ljungqvist, F.C., Büntgen, U., Zorita, E., Wagner, S., Esper, J., McCarroll, D., Toreti, A., Frank, D., Jungclaus, J.H., Barriendos, M., Bertolin, C., Bothe, O., Brázdil, R., Camuffo, D., Dobrovolný, P., Gagen, M., García-Bustamante, E., Ge, Q., Gómez-Navarro, J.J., Guiot, J., Hao, Z., Hegerl, G.C., Holmgren, K., Klimenko, V.V., Martín-Chivelet, J., Pfister, C., Roberts, N., Schindler, A., Schurer, A., Solomina, O., von Gunten, L., Wahl, E., Wanner, H., Wetter, O., Xoplaki, E., Yuan, N., Zanchettin, D., Zhang, H., Zerefos, C., 2016. European summer temperatures since Roman times. Environ. Res. Lett. 11, 024001.
47. Marchand W., Girardin M. P., Gauthier S., Hartmann H., Bouriaud O., Babst F., Bergeron Y., 2018, Untangling methodological and scale considerations in growth and productivity trend estimates of Canada's forests, Environmental Research Letters, 13 (9), 093001, doi: 10.1088/1748-9326/aad82a.
48. Mathisen I.E., Hofgaard A., 2011. Recent height and diameter growth variation in Scots pine (*Pinus sylvestris* L.) along the Arctic margin: the importance of growing season versus non-growing season climate factors. Plant. Ecol. Divers. 4, 1–11.
49. Moen A., 1999. National Atlas of Norway: vegetation. Norwegian Mapping Authority, Hønefoss.
50. NASA, 2014. National Aeronautics and Space Administration. http://modis.gsfc.nasa.gov
51. Niklas K.J., 1995. Size-dependent allometry of tree height, diameter and trunk-taper. Ann. Bot. 75 (3), 217–227. https://doi.org/10.1006/anbo.1995.1015

52. Norwegian Meteorological Institute, 2014. http://eklima.met.no
53. Oberhuber W., Swidrak I., Pirkebner D., Gruber A., 2011. Temporal dynamics of non-structural carbohydrates and xylem growth in *Pinus sylvestris* exposed to drought. Can. J. For. Res. 41, 1590–1597.
54. Ols C., Drobyshev I., Hofgaard A., Bergeron Y., 2016. Previous season climate controls the occurrence of black spruce growth anomalies in boreal forests of Eastern Canada. Can. J. For. Res. 46, 696–705.
55. Pettorelli N., Vik J.O., Mysterud A., Gaillard J.M., Tucker C.J., Stenseth N.C., 2005. Using the satellite-derived NDVI to assess ecological responses to environmental change. Trends Ecol. Evol. 20, 503–510.
56. Piao S., Wang X., Ciais P., Zhu B., Wang T.A.O., Liu J.I.E., 2011. Changes in satellite-derived vegetation growth trend in temperate and boreal Eurasia from 1982 to 2006. Glob. Chang. Biol. 17, 3228–3239.
57. Piao S., Nan H., Huntingford C., Ciais P., Friedlingstein P., Sitch S., Peng S., Ahlström A., Canadell J.G., Cong N., Levis S., Levy P.E., Liu L., Lomas M.R., Mao J., Myneni R.B., Peylin P., Poulter B., Shi X., Yin G., Viovy N., Wang T., Wang X., Zaehle S., Zeng N., Zeng Z., Chen A., 2014. Evidence for a weakening relationship between interannual temperature variability and northern vegetation activity. Nat. Comm. 5–5018.
58. Pinzon J.E., Tucker C.J., 2014. A non-stationary 1981–2012 AVHRR NDVI3g time series. Remote Sens. 6, 6929–6960.
59. Potter V.C., Brooks V., 1998. Global analysis of empirical relations between annual climate and seasonality of NDVI. Int. J. Remote Sens. 19 (15), 2921–2948. https://doi.org/10.1080/014311698214352
60. Qian H., Joseph R., Zeng N., 2010. Enhanced terrestrial carbon uptake in the Northern High Latitudes in the 21st century from the Coupled Carbon Cycle Climate Model Intercomparison Project model projections. Glob. Chang. Biol. 16, 641–656.
61. R Core Team, 2012. R: A Language and Environment for Statistical Computing. R Foundation for Statistical Computing, Vienna.
62. Raynolds M.K., Comiso J.C., Walker D.A., Verbyla D., 2008. Relationship between satellitederived land surface temperatures, arctic vegetation types, and NDVI. Remote Sens. Environ. 112, 1884–1894.
63. Roland C.A., Schmidt, J.H., Johnstone J.F., 2014. Climate sensitivity of reproduction in a mast-seeding boreal conifer across its distributional range from lowland to treeline forests. Oecologia 174**,** 665–677.

64. Salminen H., Jalkanen R., 2005. Modelling the effect of temperature on height increment of Scots pine at high latitudes. Silva Fenn, 39, 497–508.
65. Sands R., & Mulligan, D.R. 1990. Management of water and nutrient relations to increase forest growth. For. Ecol. Manage. 30(1): 91-111. doi: 10.1016/0378-1127(90)90129-Y
66. Santin-Janin H., Garel M., Chapuis J.L., Pontier D., 2009. Assessing the performance of NDVI as a proxy for plant biomass using non-linear models: a case study on the Kerguelen archipelago. Polar Biol. 32, 861–871.
67. Seftigen K., Frank D., Björklund J., Babst F., Poulter B., 2018. The climatic drivers of normalized difference vegetation index and tree-ring-based estimates of forest productivity are spatially coherent but temporally decoupled in Northern Hemispheric forests. Global Ecol. Biogeogr. 27, 1352–1365. https://doi.org/10.1111/geb.12802
68. Sendall, K.M., Reich, P.B., Zhao, C., Jihua, H., Wei, X., Stefanski, A., Rice, K., Rich, R.L., Montgomery, R.A., 2015. Acclimation of photosynthetic temperature optima of temperate and boreal tree species in response to experimental forest warming. Glob. Change Biol. 21, 1342–1357. doi:10.1111/gcb.12781
69. Solberg B.O., Hofgaard A., Hytteborn H., 2002. Shifts in radial growth responses of coastal Picea abies induced by climatic change during the 20th century, central Norway. Ecoscience 9, 79–88.
70. Stinziano J.R., Way D.A., 2014. Combined effects of rising [CO2] and temperature on boreal forests: Growth, physiology and limitations. Botany 92, 425–436.
71. Sturm M., McFadden J.P., Liston G.E., Chapin III F.S., Racine C.H., Holmgren J., 2001. Snow–shrub interactions in arctic tundra: a hypothesis with climate implications. J. Clim. 14, 336–344.
72. Tucker C.J., Pinzon J.E., Brown M.E., 2004. Global inventory modeling and mapping studies. Global Land Cover Facility, University of Maryland, Maryland.
73. Tveito O.E., Bjørdal I., Skjelvåg A.O., Aune B., 2005. A GIS-based agro-ecological decision system based on gridded climatology. Meteorol. Appl. 12, 57–68.
74. Vaganov E.A., Hughes M.K., Kirdyanov A.V., Schweingruber F.H., Silkin P.P., 1999. Influence of snowfall and melt timing on tree growth in subarctic Eurasia. Nature 400, 149–151.
75. Vaganov E.A., Anchukaitis K.J., Evans M.N., 2011. How well understood are the processes that create dendroclimatic records? A mechanistic model of the climatic control on conifer tree-ring growth dynamics. In: Hughes M.K., Swetnam T.W., Diaz H., eds. Dendroclimatology. Progress and prospects. Springer Series Development in Paleoenvironmental Research, vol. 11. Berlin/Heidelberg, Germany: Springer, 37–75.

76. Vargas R., Trumbore S.E., Allen M.F., 2009. Evidence of old carbon used to grow new fine roots in a tropical forest. New. Phytol. 182, 710–718. doi: 10.1111/j.1469-8137.2009.02789.x
77. Weier J., Herring D., 2000. Measuring Vegetation *(NDVI & EVI)*. Earth Observatory, NASA.
78. Wigley T.M.L., Briffa, K.R., Jones P.D., 1984. On the average value of correlated time series, with applications in dendroclimatology and hydrometeorology. J. Clim. Appl. Meteorol. 23, 201–213.
79. Zang C., Biondi F., 2015. treeclim: an R package for the numerical calibration of proxy-climate relationships. Ecography 38(4), 431–435.
80. Zhou L., Kaufmann R.K., Tian Y., Myneni R.B., Tucker C.J., 2003. Relation between interannual variations in satellite measures of northern forest greenness and climate between 1982 and 1999. J. Geophys. Res. 108 (D1), ACL 3-1–ACL 3-16. 10.1029/2002JD002510

Figures

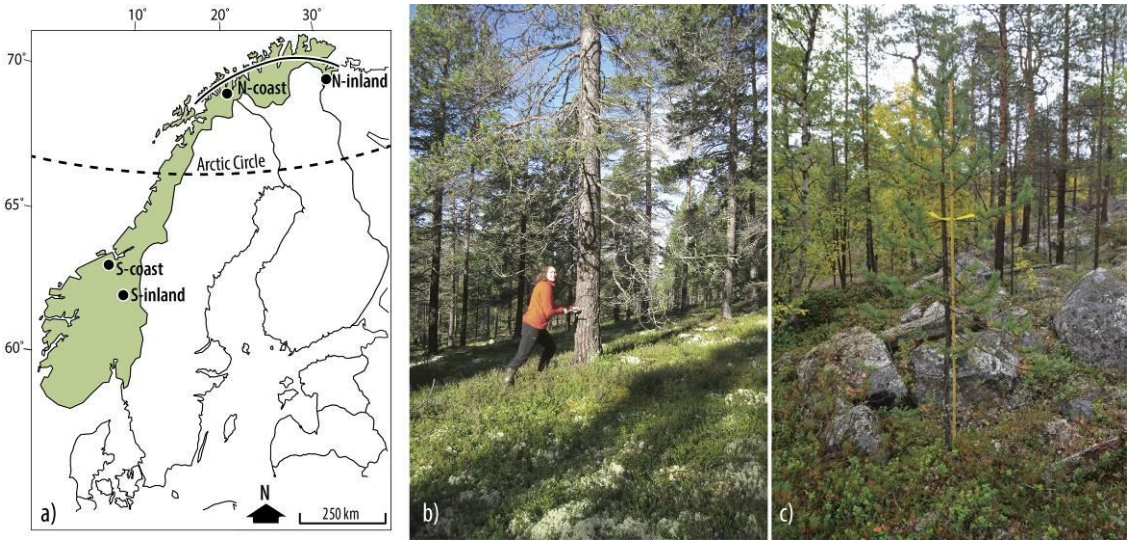

Fig. 1 Sampling site locations across Norway (panel a): Takvan (N-coast), Pasvik (N-inland), Songli (S-coast), and Atna (S-inland). The black continuous line across northern Norway indicates approximate position of northernmost Scots pine forests. Panels b) and c) show examples of an adult Scots pine selected for radial growth analysis and a young Scots pine selected for height growth analysis, respectively. For more information regarding sampling sites characteristics (e.g. coordinates and mean climate) please see Table S1.

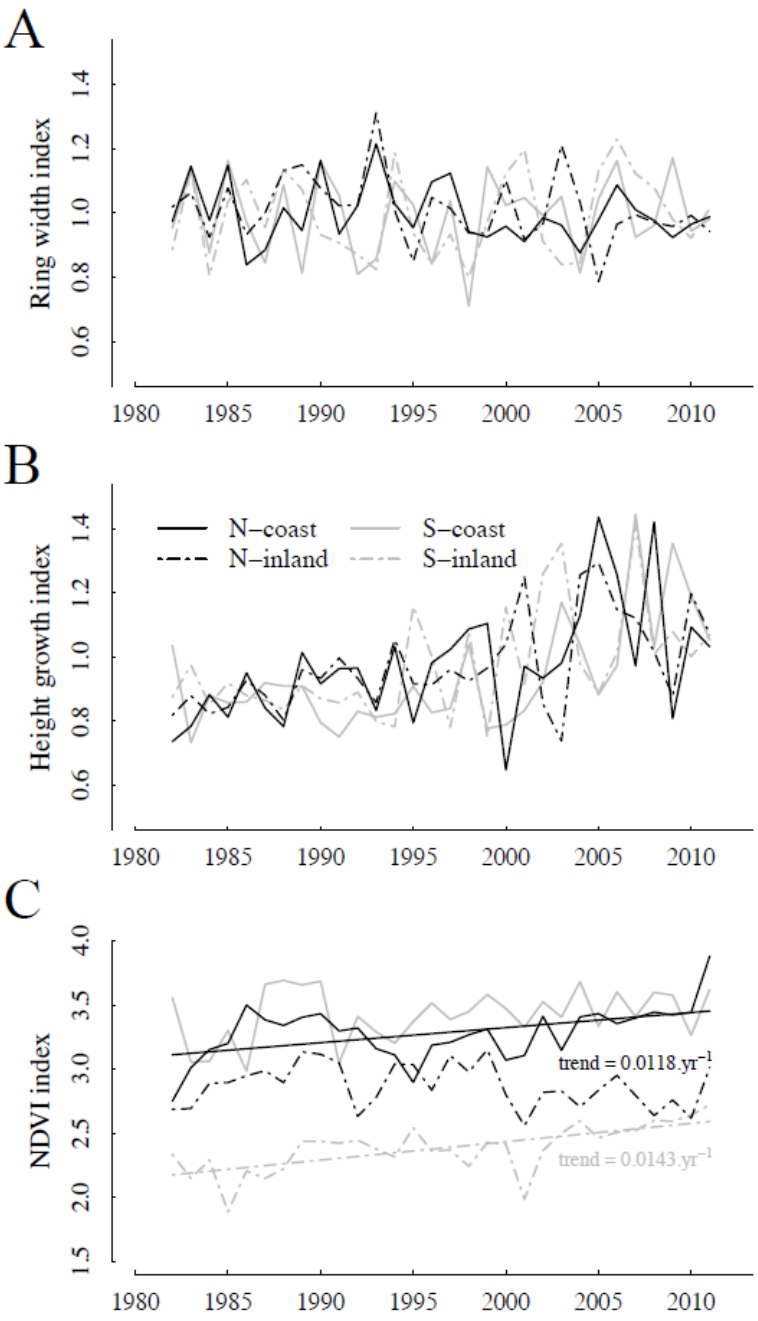

Fig. 2 Standardized chronologies for radial growth (A), height growth (B), and cumulative May to September NDVI (C) for the four sampling sites over the 1982-2011 period. Significant positive trends in cumulative NDVI ($P < 0.05$) identified at N-coast (+0.0118.yr^{-1}) and at S-inland (+0.0143.yr^{-1}) are plotted.

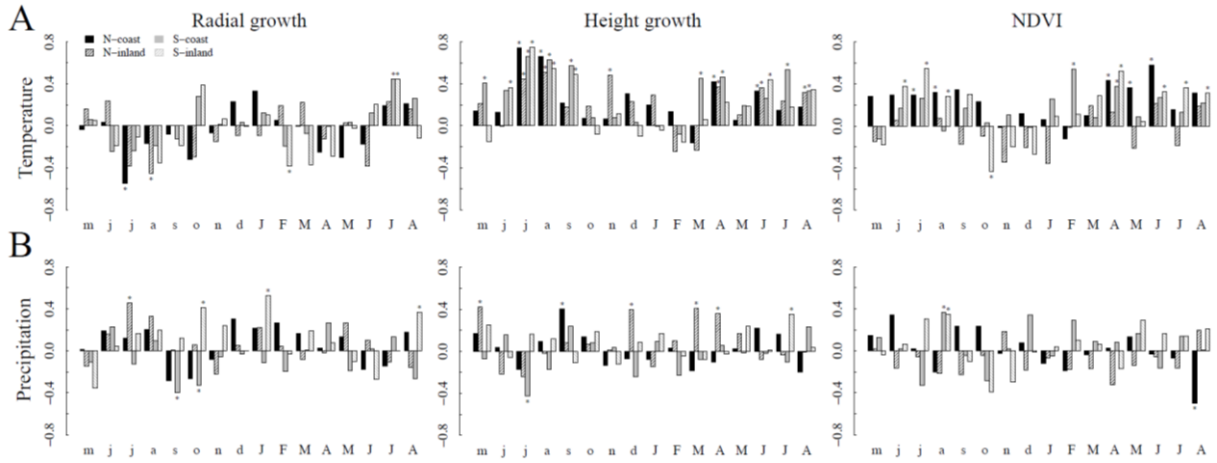

Fig. 3 Correlations between temperature (a) and precipitation (b), and radial growth (left-hand panels), height growth (central panels), and cumulative NDVI (right-hand panels) indices as revealed by Pearson correlations. Analyses cover the 1982-2011 period. The analyses include months from May the year prior to growth to August the year of growth. Significant values ($P < 0.05$), established through bootstrapping procedures, are indicated with a star (*). Uppercases indicate current year months and lowercases previous year months.

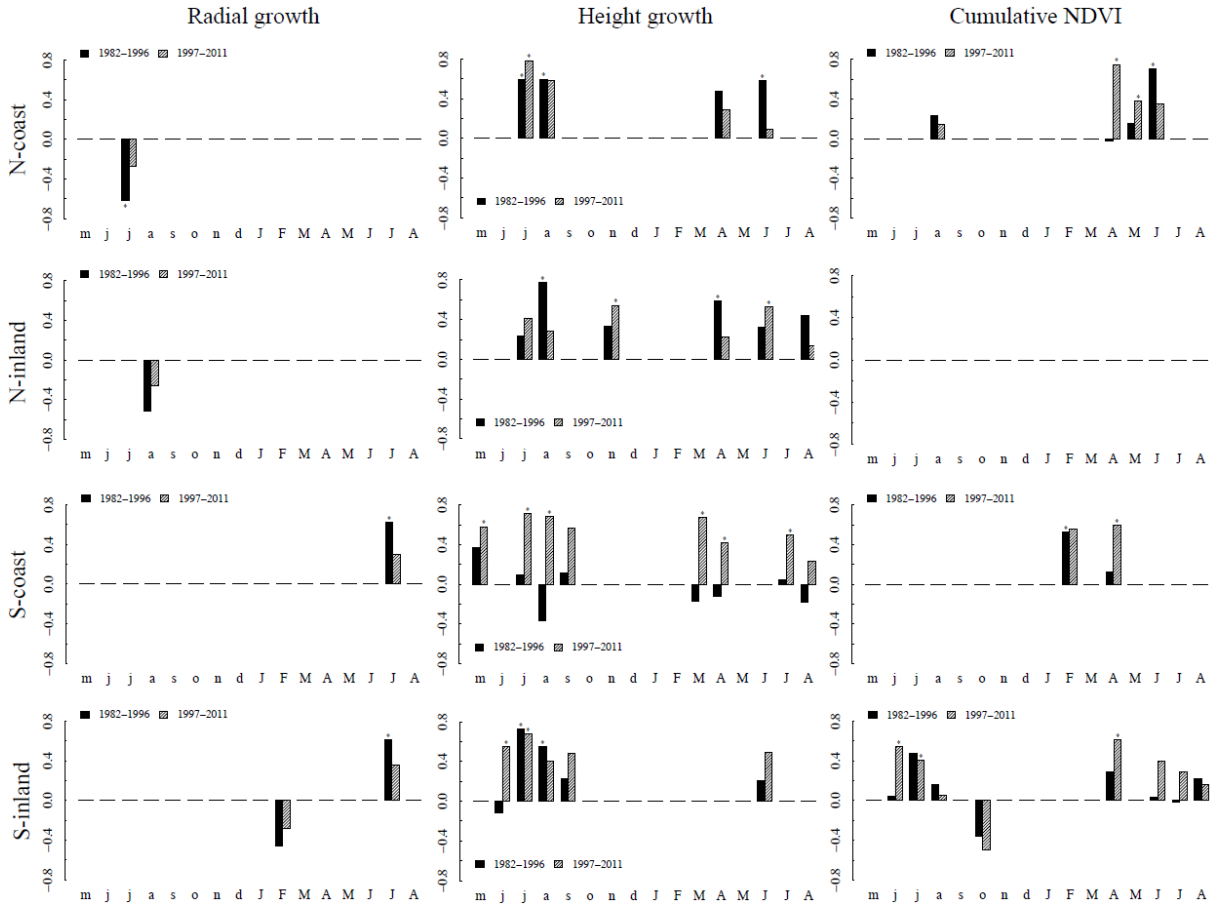

Fig. 4 Temporal variations in correlations between temperature and forest productivity proxies (radial growth, height growth and cumulative NDVI), as revealed by bootstrapped correlations. Correlations were computed over two 15-yr periods, the 1982-1996 and the 1997-2011 period. Only months with significant correlation over the 1982-2011 period (see Fig. 3) are plotted. Uppercases indicate current year months and lowercases previous year months. Significant correlations ($P < 0.05$) are indicated by a star (*).

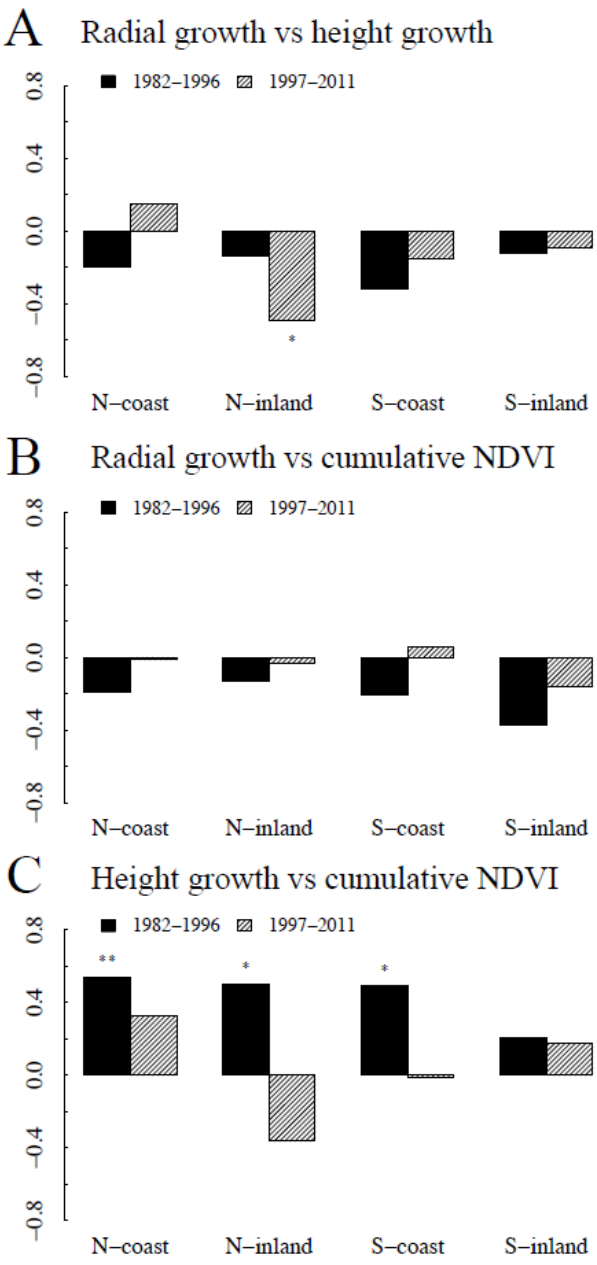

Fig. 5 Correlations between forest productivity proxies (radial growth, height growth, and cumulative NDVI) revealed by bootstrapped correlations. Correlations were computed over two 15-yr periods, the 1982-1996 and the 1997-2011 period. Significant correlations are indicated by * (P < 0.1) and ** (P < 0.05).

Tables

Table 1. Summary statistics for radial and height growth data. Statistics were computed over the 1982-2011 period.

	N-coast	**N-inland**	**S-coast**	**S-inland**
Radial growth				
Number of trees*	30 (30)	30 (30)	30 (29)	30 (30)
Number of cores*	60 (60)	60 (59)	55 (55)	57 (57)
Mean tree-ring width (mm)	1.08	1.68	0.65	0.72
Mean series length (years)	95 ±30	62 ±10	115 ±37	133 ±35
Mean correlation between series	0.24	0.35	0.41	0.48
Expressed population signal (EPS)	0.91	0.94	0.95	0.97
Signal to noise ratio (SNR)	9.7	15.8	19.8	27.3
Height growth				
Number of trees*	25 (10)	24 (15)	31 (10)	17 (10)
Mean annual growth (cm)	8.98	9.05	8.25	8.91
Mean series length (years)	29 ±5	31 ±4	25 ±7	31 ±3
Mean correlation between series	0.32	0.23	0.25	0.18
Expressed population signal (EPS)	0.89	0.87	0.89	0.77
Signal to noise ratio (SNR)	8.3	6.7	7.9	3.3

*values in brackets give the minimum sample depth over the 1982-2011 period.

Table 2. Site-specific correlations between the three forest productivity proxies (radial growth, height growth, and cumulative NDVI (May-September)). Correlations are calculated over the 1982-2011 period. Significant correlations are indicated by asterisks (** - $P < 0.05$; *- $P < 0.1$).

	N-coast	**N-inland**	**S-coast**	**S-inland**
Radial vs. Height	-0.13	-0.44**	-0.12	-0.02
Radial vs. NDVI	-0.19	-0.04	-0.08	-0.18
Height vs. NDVI	0.47**	-0.21	0.27	0.34*

SUPPLEMENTARY MATERIAL

Spatiotemporal variation of the correspondence between boreal forest productivity proxies and climate data

C. Ols, I. H. Kålås, I. Drobyshev, L. Söderström, A. Hofgaard

Content:

APPENDIX A - SITE-SPECIFIC CHARACTERISTICS

Table S1. Characteristics of the four sampling sites. Climate metrics are based on 1982-2011 grid data from the Norwegian Meteorological Institute (http://eklima.met.no). Average NDVI were computed over the 1982-2011 period using raw data from the NASA MODIS project (http://modis.gsfc.nasa.gov 2014). Abbreviations: DJF-December to February; JJA:-June to August, O1 = slightly oceanic section, O2 = markedly oceanic section; C1 = slightly continental section. *According to Moen 1999. # According to the geological survey of Norway http://geo.ngu.no/kart/berggrunn_mobil/?lang=eng.

	N-coast	**N-inland**	**S-coast**	**S-inland**
Elevation (m a.s.l.)	150	170	270	730
Latitude (N)	69°10'	69°17'	63°19'	61°53'
Longitude (E)	19°12'	29°08'	9°39'	10°08'
Annual temperature, °C	1.7	-0.5	3.3	0.2
Winter (DJF) temp., °C	-6.6	-11.2	-3.4	-9.8
January temp., °C	-6.9	-11.8	-3.5	-10.1
Summer (JJA) temp., °C	11.4	10.7	11.1	10.7
July temp., °C	12.8	12.5	12.1	12.0
Annual precipitation, mm	934	515	1795	771
Summer (JJA) prec., mm	216	198	367	304
Number of days >5 °C*	140	120	190	140
NDVI (average May-Sept.)	0.65	0.57	0.68	0.48
Vegetation section*	O1	C1	O2	C1
Geological substrate#	sand shale	granite gneiss, migmatite	charnockite, anorthosite	metasandstone, schist

Table S2. Trends in seasonal mean temperature and total precipitation at the four sampling sites over the 1982-2011 period, based on 1km^2 site-centered grid data from the Norwegian Meteorological Institute (http://eklima.met.no). Trends were calculated by linear regression of climate metrics by time. R-squared (r^2) and slope of each linear regression are presented for each seasonal climate metric. Seasons were define as follow: Winter -December to February; Spring-March to May; Summer-June to August; Autumn-September to November. Significance levels: * $P < 0.05$;** $P < 0.01$;*** $P < 0.001$.

	N-coast	N-inland	S-coast	S-inland
Temperature				
Winter				
slope	0.07	0.04	0.07	-0.05
r^2	0.05	-0.02	0.02	-0.002
Spring				
Slope	0.05	0.05	0.07	0.01
r^2	0.09	0.04	0.24**	-0.03
Summer				
slope	0.06	0.04	0.07	0.08
r^2	0.30***	0.15*	0.29**	0.34***
Autumn				
slope	0.07	0.06	0.06	0.002
r^2	0.18*	0.12*	0.11*	-0.04
Precipitation				
Winter				
slope	-0.42	0.54	-1	0.83
r^2	-0.03	0.007	-0.003	0.003
Spring				
slope	2.15	1.28	0.27	0.55
r^2	0.04	0.26***	-0.04	-0.017
Summer				
slope	-0.007	-1.07	1.26	5.13
r^2	-0.04	-0.004	-0.01	0.36***
Autumn				
slope	-1.02	0.40	-2.04	-0.19
r^2	-0.03*	-0.02	-0.03	-0.03

Table S3. Coherence between grid data from the Norwegian Meteorological Institute (http://eklima.met.no) and closest meteorological station data for the four sampling sites over the 1982-2011 period. Site distance to meteorological station and mean Pearson correlation (r) between both types of climate data over all monthly variables are presented. For all sites, except N-coast, the nearest climate stations for temperature and precipitation differ because most selected stations either record one climatic parameter or the other.

	N-coast	**N-inland**	**S-coast**	**S-inland**
Temperature				
Reference meteorological station	Bardufoss	Kirkenes	Ørland	Fokkstugu
Distance site-station (km)	23	70	58	70
r	0.994	0.998	0.990	0.990
Precipitation				
Reference meteorological station	Bardufoss	Skogfoss	Songli	Atnasjøen
Distance site-station (km)	23	33	20	40
r	0.907	0.930	0.980	0.976

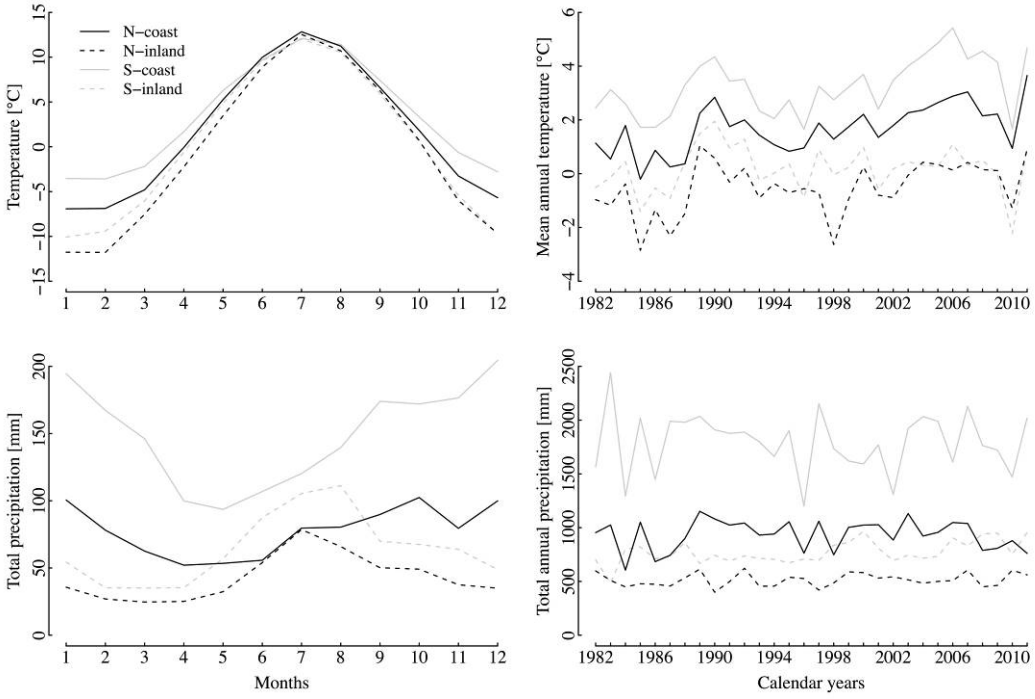

Figure S1. Temperature and precipitation grid data at the four sampling sites over the 1982-2011 period. Average monthly mean temperature (left-hand panel) and annual mean temperature (right-hand panel). Average monthly total precipitation (left-hand panel) and annual total precipitation (right-hand panel). Grid data were retrieved from the Norwegian Meteorological Institute (http://eklima.met.no).

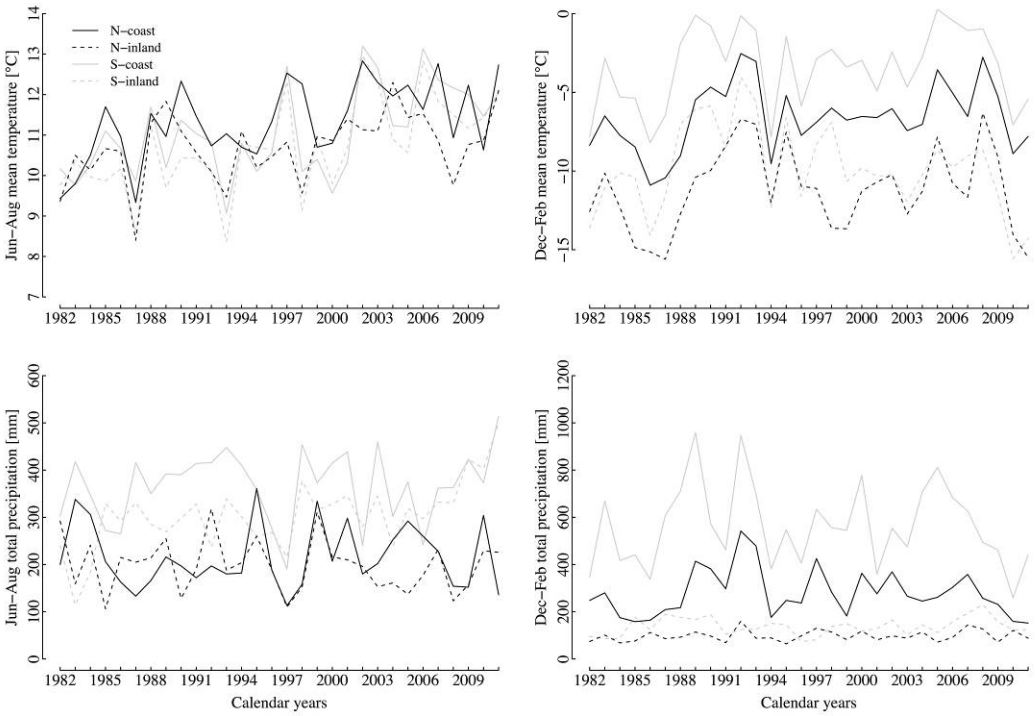

Figure S2. Summer and winter mean temperature (top panels) and total precipitation (bottom panels) for the 1982-2011 period. Summer (JJA) and winter (DJF) values are shown in the left- and right-hand panels respectively. Grid data was retrieved from the Norwegian Meteorological Institute (http://eklima.met.no).

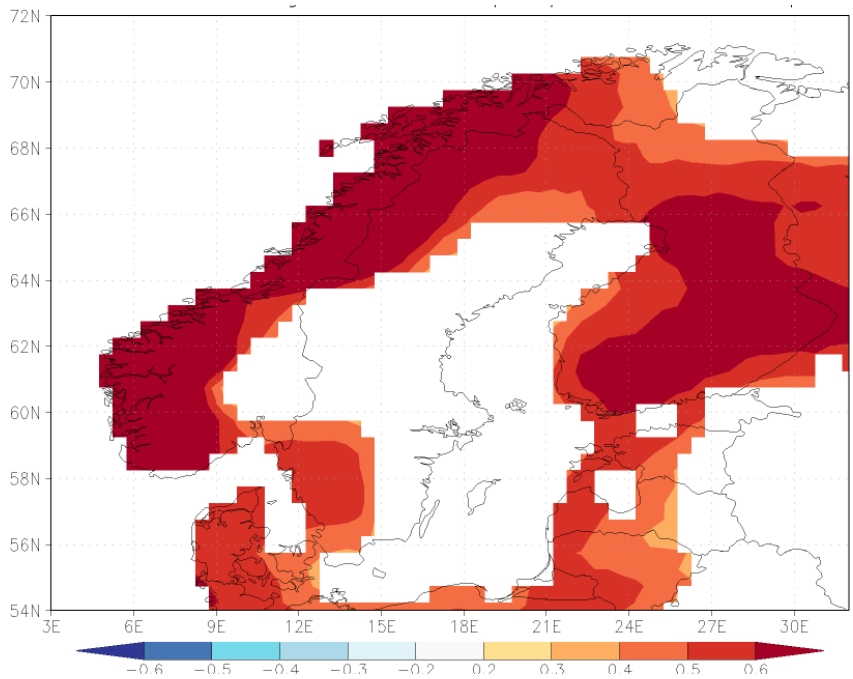

Figure S3. Point-wise correlation between winter (December through February) temperature averages and precipitation sums in the study area. Correlations were computed over the 1982-2011 period using the 0.5°lat. x 0.5° lon. CRU TS 4.01 data set in Climate explorer (https://climexp.knmi.nl). Only significant correlations ($P < 0.05$) are plotted.

APPENDIX B - EFFECTS OF THREE DIFFERENT DETRENDING METHODS ON TREE GROWTH PATTERNS AND TREE GROWTH RESPONSES TO CLIMATE

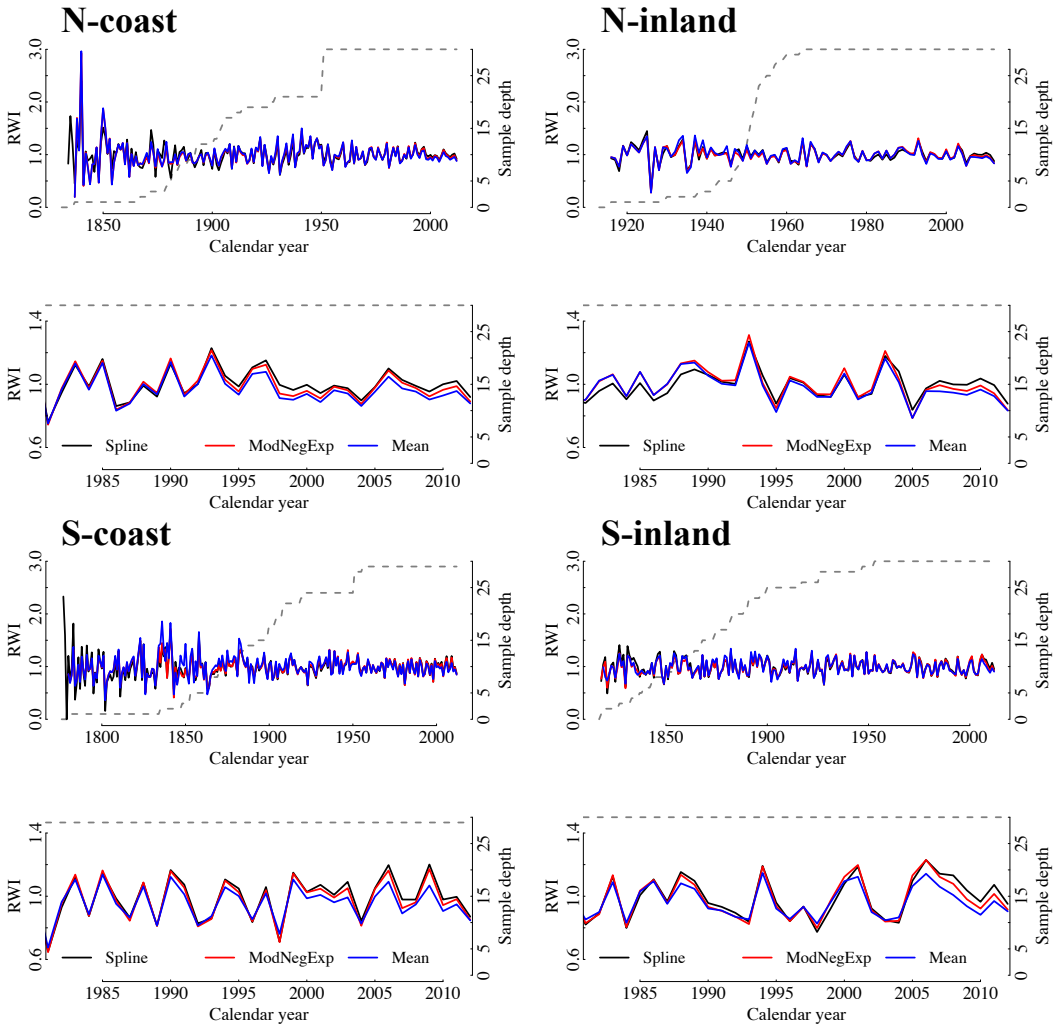

Figure S4. Application of three different detrending methods on radial growth series. Radial growth series were first detrended using three different methods, with residuals computed as ratios, and then pre-whitened (autocorrelation removal). Detrending was performed on the total length of each series. The three detrending methods implemented were a 67% smoothing spline (“Spline”, black line), a modified negative exponential curve (“ModNegExp”, red line), and a simple horizontal line ("Mean", blue line). The sample depth axis indicates the number of trees used to compute the site-specific master chronology for each calendar year. Lower panels depict the difference between series over the 1982-2011study period.

Table S4. Site-specific Pearson correlation between the three types of detrended radial series over 1982-2011. The three detrending methods implemented were a 67% smoothing spline (“Spline”), a modified negative exponential curve (“ModNegExp”), and a simple horizontal line ("Mean"). All correlations were significant ($P < 0.05$).

Sampling site	N-coast	N-inland	S-coast	S-inland
Mean vs Spline	0.95	0.91	0.96	0.95
ModNegExp vs Spline	0.97	0.94	0.99	0.98
Mean vs ModNegExp	0.99	0.99	0.98	0.99

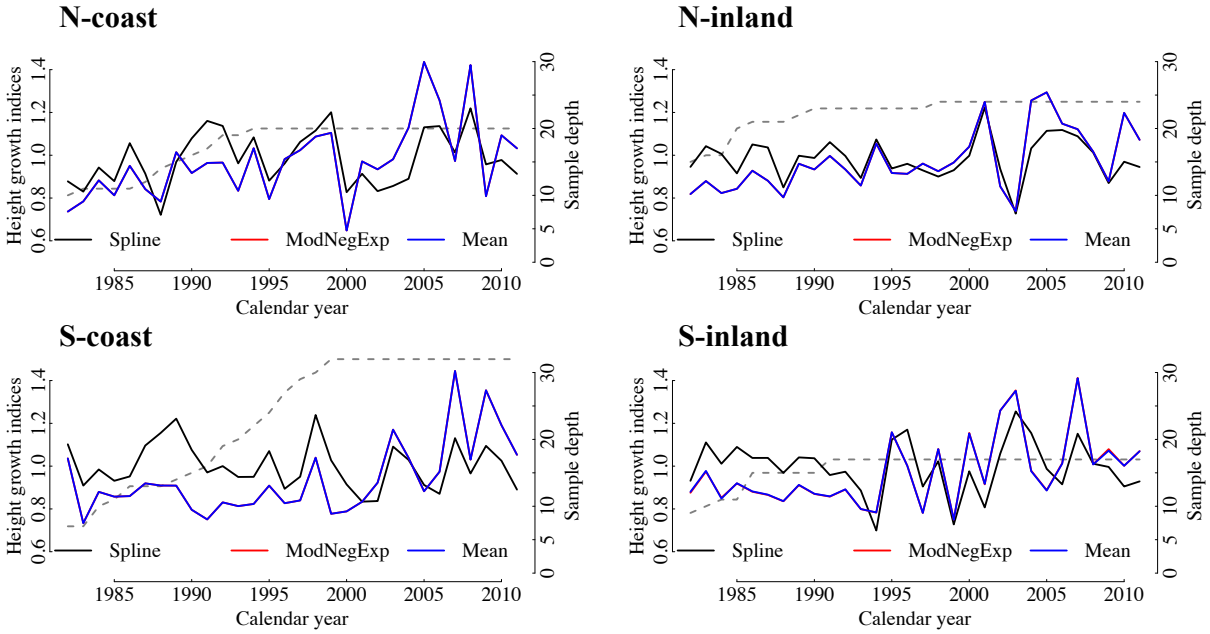

Figure S5. Application of three different detrending methods on height growth series, displayed with one panel per site. Panels display the obtained detrended series over the 1982-2011period. The three detrending methods implemented were a 67% smoothing spline ("Spline", black line), a modified negative exponential curve ("ModNegExp", red line), and a simple horizontal line ("Mean", blue line). The sample depth axis indicates the number of trees used to compute the site-specific master chronology for each calendar year. Please note that the Mean and ModNegExp curves at most sites are exactly similar (see Table S2), therefore only two curves are depicted.

Table S5. Site-specific Pearson correlation between the three types of detrended height growth series over the 1982-2011 period. The three detrending methods implemented were a 67% smoothing spline ("Spline"), a modified negative exponential curve ("ModNegExp"), and a simple horizontal line ("Mean"). All correlations were significant ($P < 0.05$), except between the ModNegExp and Mean chronology on one side, and the Spline chronology on the other side at S-coast.

Sampling site	N-coast	N-inland	S-coast	S-inland
Mean vs Spline	0.69	0.71	0.42	0.61
ModNegExp vs Spline	0.69	0.71	0.42	0.61
Mean vs ModNegExp	1	1	1	0.99

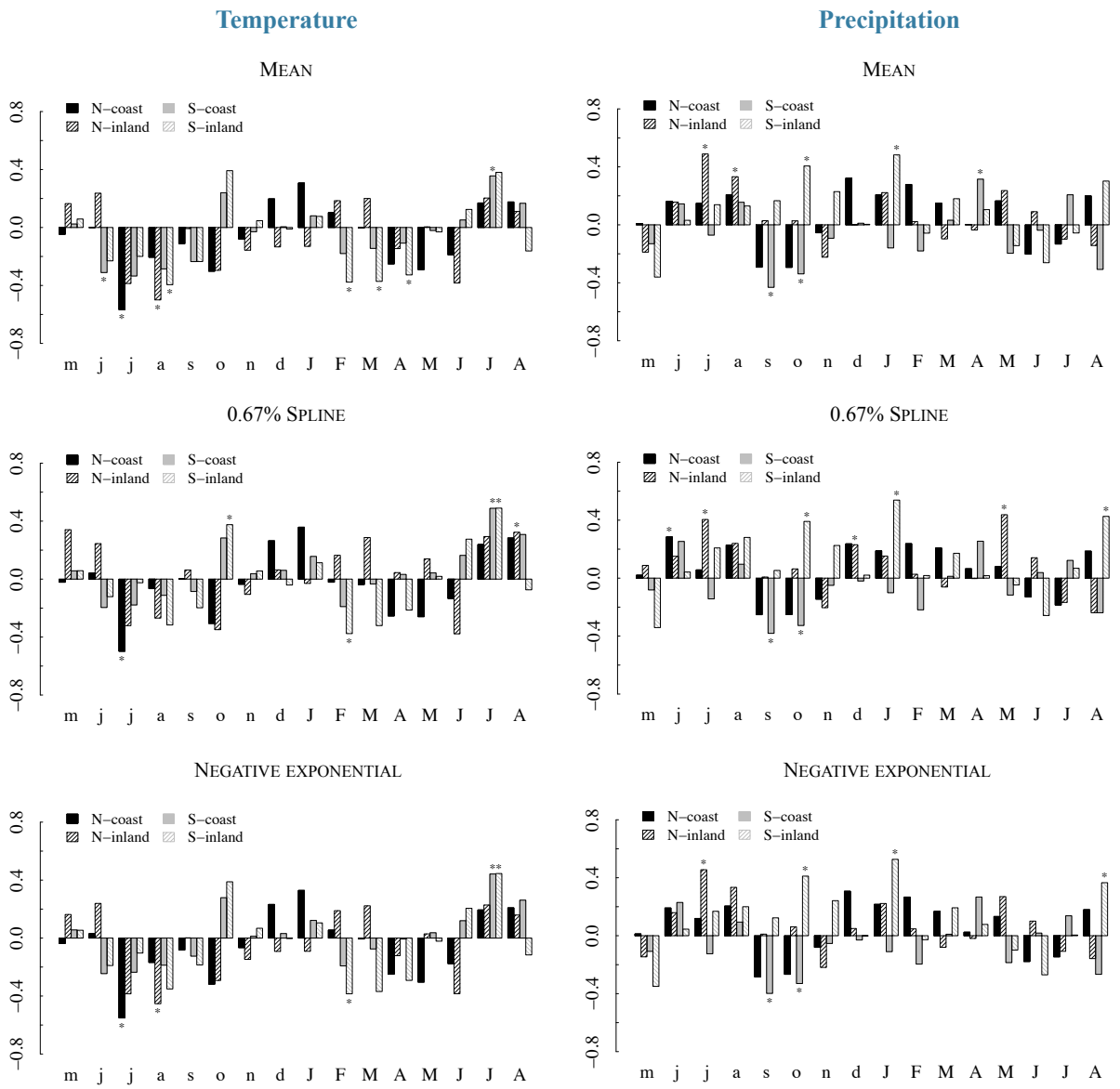

Figure S6. Correspondence between temperature (left panels) and precipitation (right panels), and radial growth indices as revealed by Pearson correlations. Radial growth indices were obtained using three different detrending methods: a simple horizontal line (upper panel), a 67% smoothing spline (middle panel), and a modified negative exponential curve (lower panel). Analyses cover the 1982-2011 period. The analyses include months from May the year prior to growth to August the year of growth. Significant values ($P < 0.05$), established through bootstrapping procedure, are indicated with a star (*). Uppercases indicate current year months and lowercases previous year months.

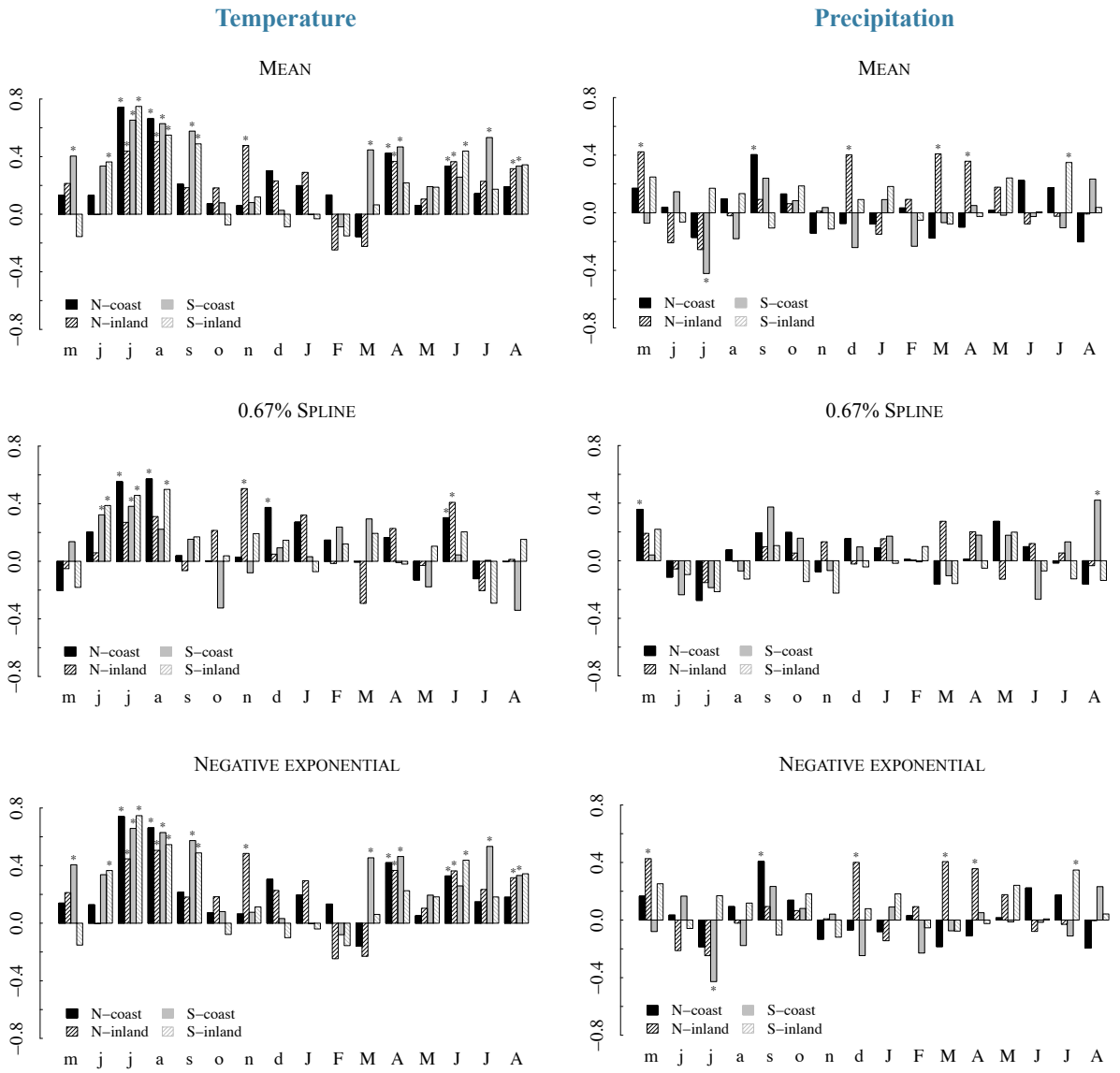

Figure S7. Correspondence between temperature (left panels) and precipitation (right panels), and height growth indices as revealed by Pearson correlations. Height growth indices were obtained using three different detrending methods: a simple horizontal line (upper panel), a 67% smoothing spline (middle panel), and a modified negative exponential curve (lower panel). Analyses cover the 1982-2011 period. The analyses include months from May the year prior to growth to August the year of growth. Significant values ($P < 0.05$), established through bootstrapping procedure, are indicated with a star (*). Uppercases indicate current year months and lowercases previous year months.

APPENDIX C - TREE-RING CHRONOLOGIES AND CLIMATE-GROWTH RESPONSES

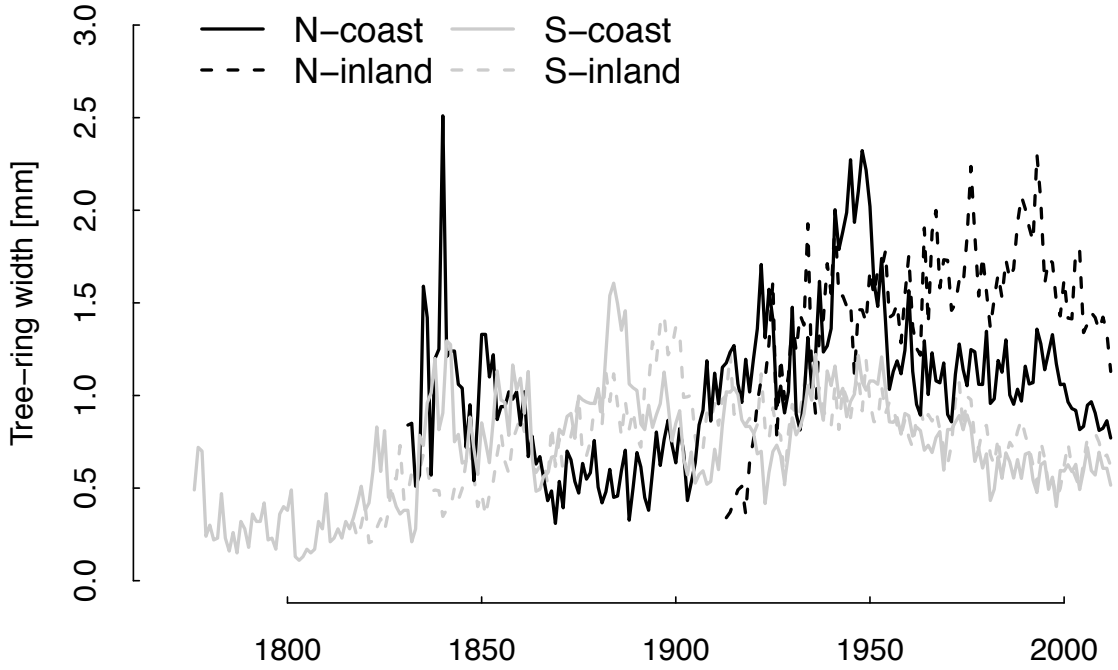

Figure S8. Mean tree-ring width chronologies at the four sampling sites obtained from the complete measurements of 10 radial series at each site. Ring-width measurements primarily covered the 1982-2011 period but at least ten trees per site were measured along total core length. The number of trees included in each site-specific chronology over the 1982-2011 period in given in Table 1. See Fig. 1 for study site locations and Table S1 for site characteristics. Trees at northern sites were younger than in the south and had a larger mean ring width (northern mean 1.31 mm, southern mean 0.6 mm).

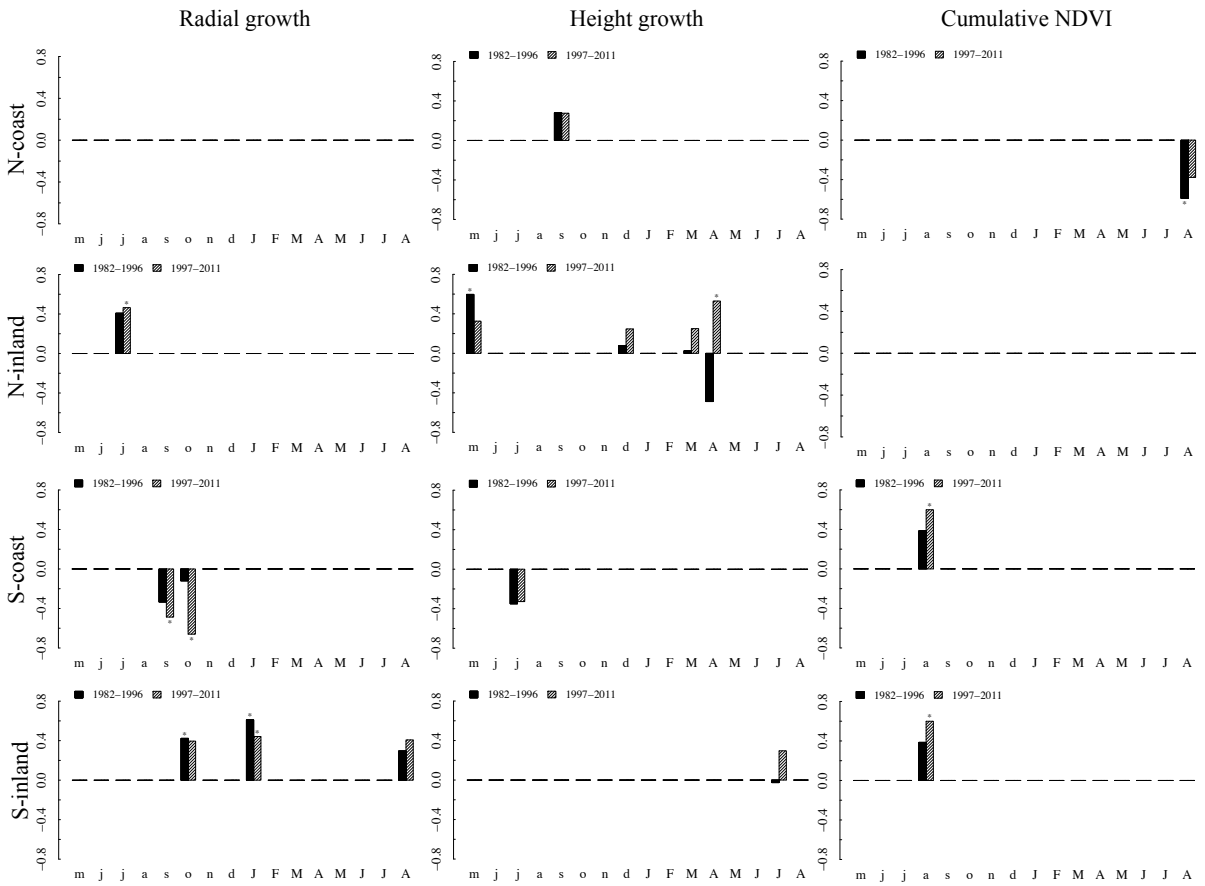

Figure S9. Temporal variations in correlations between precipitations and forest productivity proxies (radial growth, height growth and cumulative NDVI), as revealed by bootstrapped correlations. Correlations were computed over two 15-yr periods, the 1982-1996 and the 1997-2011 period. Only months with significant correlation over the 1982-2011 period (see Fig. 3) are plotted. Uppercases indicate current year months and lowercases previous year months. Significant correlations ($P < 0.05$) are indicated by a start (*).

APPENDIX D – RADIAL AND HEIGHT GROWTH VS. MONTHLY NDVI

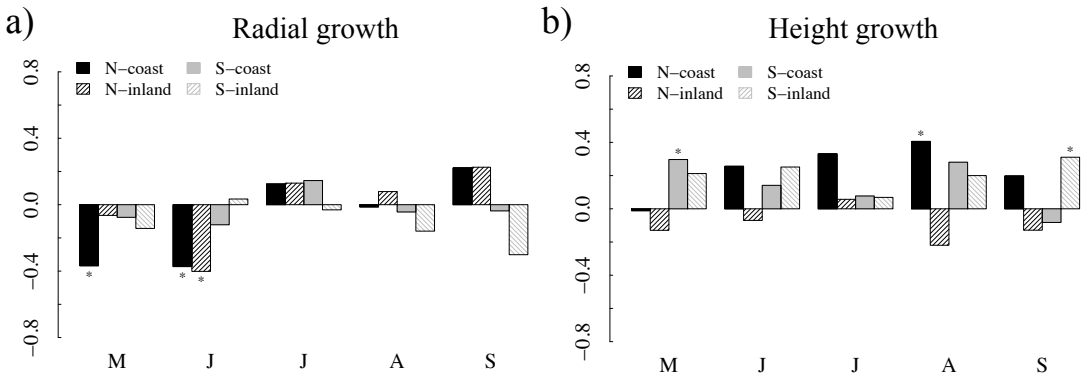

Figure S10. Correspondence between monthly NDVI and radial growth (a) and height growth (b) indices over the 1982-2011 period as revealed by bootstrapped correlation analyses. Monthy NDVI includes individual months from May (M) to September (S) in the year of growth. Significant correlations ($P < 0.05$) are marked with a start (*).

APPENDIX E – COHERENCY OF PROXIES THROUGH SPACE

Table S6. Between-site correlations for the three forest productivity proxies (radial, height and cumulative NDVI (May-September) data). Analyses cover the 1982-2011 period. Significant correlations are indicted by asterisks (* $P < 0.05$; ** $P < 0.01$). Correlations between sites for each proxy were only significant between S-coast and S-inland (r = 0.48) for radial growth (Table 1), between S-coast and S-inland (r = 0.43), N-coast and N-inland (r = 0.52) for height growth (Table 1), and between N-coast and S-inland (r = 0.40) for cumulative NDVI (Table 1).

	N-coast	**N-inland**	**S-coast**	**S-inland**
Radial growth				
N-inland	0.46**			
S-coast	0.25	-0.09		
S-inland	-0.01	-0.20	0.52**	
Height growth				
N-inland	0.60**			
S-coast	0.13	0.12		
S-inland	-0.05	0.001	0.64**	
NDVI				
N-inland	0.17			
S-coast	0.28	0.10		
S-inland	0.40*	0.00	0.33	

APPENDIX F – EFFECT OF DETRENDING NDVI INDICES ON CLIMATE-PROXY AND PROXY-PROXY RELATIONSHIPS

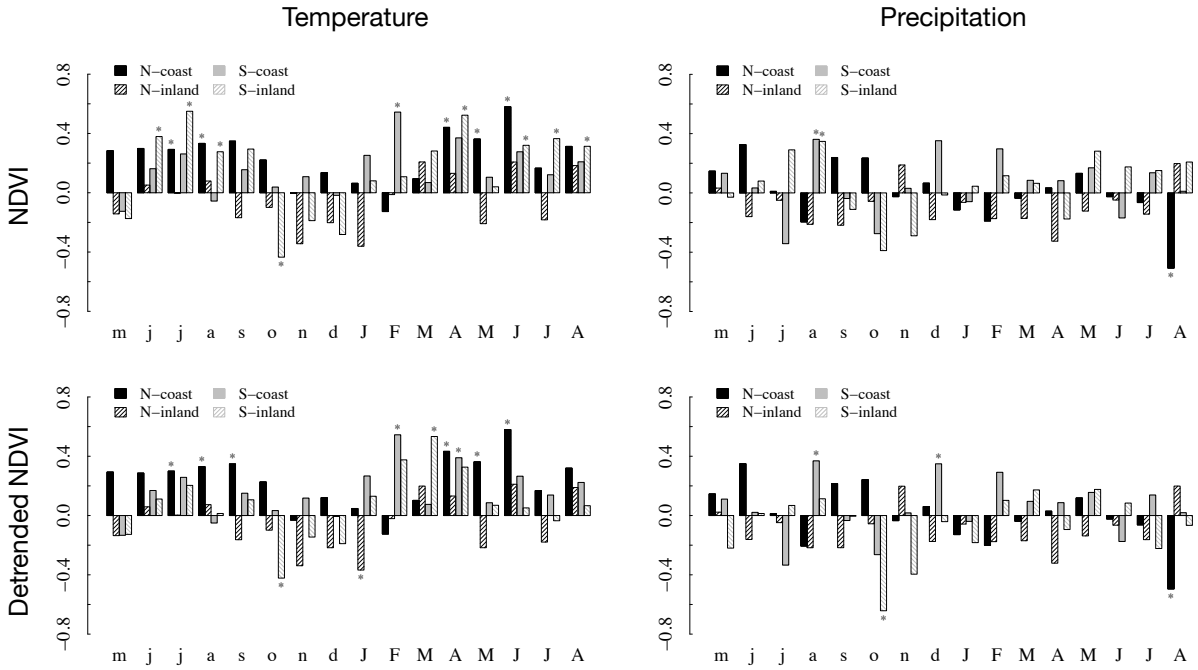

Figure S11. Correspondence between cumulative NDVI and monthly temperature (left panels) and precipitation (right panels) over the 1982-2011 period as revealed by bootstrapped correlation analyses. Cumulative NDVI includes months from May (M) to September (S) in the year of growth. Significant correlations ($P < 0.05$) are marked with a start (*).

Table S7. Effects of detrending cumulative NDVI (May-September) series on the correspondence between NDVI series and radial and height growth. Correlations are calculated over the 1982-2011 period. Significant correlations at $P < 0.05$ are indicated by asterisks *.Correlations obtained using undetrended NDVI series are presented in brackets.

	N-coast	**N-inland**	**S-coast**	**S-inland**
Radial vs NDVI det	-0.11 (-0.19)	-0.10 (-0.04)	-0.10 (-0.08)	-0.35 (-0.18)
Height vs NDVI det	0.23 (0.47)	-0.08 (-0.21)	0.09 (0.27)	-0.003 (0.34)